HAAR WAVELETS SCHEME FOR SOLVING THE UNSTEADY GAS-FLOW IN 4-D

by

Mohamed R. ALI[a*] and Dumitru BALEANU[b,c]

[a] Department of Mathematics, Benha Faculty of Engineering,
Benha University, Benha, Egypt
[b] Department of Mathematics, Cankaya University, Ankara, Turkey
[c] Institute of Space Sciences, Magurele, Romania

Original scientific paper
https://doi.org/10.2298/TSCI190101292A

The system of unsteady gas-flow of 4-D is solved successfully by alter the possibility of an algorithm based on collocation points and 4-D Haar wavelet method. Empirical rates of convergence of the Haar wavelet method are calculated which agree with theoretical results. To exhibit the efficiency of the strategy, the numerical solutions which are acquired utilizing the recommended strategy demonstrate that numerical solutions are in a decent fortuitous event with the exact solutions.

Key words: *Haar wavelets, a system of 4-D unsteady gas-flow, stability analysis, error analysis*

Introduction

Haar wavelets are the most basic ones which are defined by an investigative articulation. Because of their straightforwardness, the Haar wavelet method (HWM) is extremely powerful instruments for approximating arrangements of PDE. The wavelets are utilized as a scientific device for taking care of many classes of equations in biology, physics, fluid mechanics, and chemical reactions. This technique comprises of diminishing the issue to a lot of arithmetical conditions by growing the term which has the greatest subsidiary, given in the condition as Haar wavelets with obscure coefficients.

The solution of the system of 4-D unsteady gas-flow problem under the reasonable initial condition is an essential field of study. The solutions of the unsteady gas-flow are contemplated in writing and are explained by the different strategies [1-6]. A standout amongst the most amazing strategies to decide solutions for non-linear PDE is the HWM [7-12]. Hence, utilizing this technique over and over and with the assistance of closeness factors, we can lessen the arrangement of PDE to an arrangement of ODE, which is by and large non-linear. Now and again, it is conceivable to fathom these ODE to decide the estimate arrangements; non-etheless, much of the time the ODE must be illuminated numerically. Utilizations of this technique for temperamental 1-D issues might be found in [13]. In [14] they built up a new homotopy perturbation strategy (NHPM) to get arrangements of the frameworks of non-linear partial differential equations (NPDE). In [15] they proposed another homotopy analysis scheme to obtain solutions of the systems of NPDE. In [16] scheme of reduced differential transform method

* Corresponding author, e-mail: mohamed.reda@bhit.bu.edu.eg

(RDTM) is used to the systems of NPDE and there are many methods for solving systems of partial differential equations [17-24].

In this paper, we extend the Haar wavelets scheme to solve the unsteady gas-flow in 4-D then, analysis of the increase or decrease velocity components throughout the increment of the adiabatic index.

Model formulation of the problem

The governing equations describing the unsteady gas-flow in 4-D are formulated from the general Navier-Stokes equations and Raja *et al.* work [25] on the following form:+

$$\begin{gathered}
\frac{\partial \rho}{\partial t}+\rho\left(\frac{\partial L}{\partial x}+\frac{\partial M}{\partial y}+\frac{\partial N}{\partial z}\right)+L\frac{\partial \rho}{\partial x}+M\frac{\partial \rho}{\partial y}+N\frac{\partial \rho}{\partial z}=0\\
\frac{\partial L}{\partial t}+L\frac{\partial L}{\partial x}+M\frac{\partial L}{\partial y}+N\frac{\partial L}{\partial z}+\frac{1}{\rho}\frac{\partial P}{\partial x}=0\\
\frac{\partial M}{\partial t}+L\frac{\partial M}{\partial x}+M\frac{\partial M}{\partial y}+N\frac{\partial M}{\partial z}+\frac{1}{\rho}\frac{\partial P}{\partial y}=0\\
\frac{\partial N}{\partial t}+M\frac{\partial N}{\partial x}+N\frac{\partial N}{\partial y}+N\frac{\partial N}{\partial z}+\frac{1}{\rho}\frac{\partial P}{\partial z}=0\\
\frac{\partial P}{\partial t}+P\left(\frac{\partial L}{\partial x}+\frac{\partial M}{\partial y}+\frac{\partial N}{\partial z}\right)+L\frac{\partial P}{\partial x}+M\frac{\partial P}{\partial y}+N\frac{\partial P}{\partial z}=0
\end{gathered} \tag{1}$$

where x, y, z are the space co-ordinates, t – the time, P – the pressure, ρ – the density, γ – the adiabatic index and L, M, and N the velocity components in the x-, y-, and z-directions, respectively.

There are a few endeavors to explain frameworks of NPDE.

Haar wavelet method

Haar wavelet is a successful instrument to tackle many issues emerging in numerous regions of sciences. Usually, the Haar wavelets are defined for the interval $x \in [0, 1]$ however in general case $x \in [a, b]$ one can divide the interval into m equal subintervals each of width $\Delta x = (b - a)/\mathrm{m}$. The Haar wavelets family $\{h_i(\mathrm{x})\}$ is defined as a gathering of symmetrical square waves with greatness ± in some intervals and zero elsewhere:

$$h_i(x)=\begin{cases}1, & \alpha<x<\beta\\ -1, & \beta<x<\chi\\ o, & \text{elsewhere}\end{cases} \tag{2}$$

where

$$\alpha=\frac{k}{m},\ \beta=\frac{k+0.5}{m},\ \chi=\frac{k+1}{m} \tag{3}$$

The integerdenote the wavelet level, an $m = 2^j$ where $j = 0, 1, 2,..., J$, denote the wavelet level, and $k = 0, 1, 2,..., m - 1$ is denote the translation parameter. Resolution level is known as the integer J. The index i established according to the formula $i = m + k + 1$. In case of the values $m = 1$, $k = 0$, we own $i = 2$. The value of i is $i = 2M = 2^{J+1}$. So, the integrable function $f(x)$ characterized on [0, 1) as a finite sum:

$$f(x) = \sum_{i=1}^{N} a_i h_i(x)$$

To solve PDE of any order, we need the following integrals:

$$P_{i,1}(t) = \int_0^t h_i(T)\,\mathrm{d}T \tag{4}$$

$$P_{i,n+1}(t) = \int_0^t P_{i,n}(T)\,\mathrm{d}T,\ n = 1,2,\ldots \tag{5}$$

Using eqs. (2), (4), and (5) we have:

$$P_{i,1}(t) = \begin{cases} t-\alpha, & t \in [\alpha,\beta) \\ -t, & t \in [\beta,\chi) \\ o, & \text{elsewhere} \end{cases} \tag{6}$$

$$P_{i,2}(t) = \begin{cases} \dfrac{1}{2}(t-\alpha)^2, & t \in [\alpha,\beta) \\ \dfrac{1}{4m^2} - \dfrac{1}{2}(\chi - t)^2, & t \in [\beta,\chi) \\ \dfrac{1}{4m^2}, & t \in [\chi,1) \\ o, & \text{elsewhere} \end{cases} \tag{7}$$

$$P_{i,3}(t) = \begin{cases} \dfrac{1}{6}(t-\alpha)^3, & t \in [\alpha,\beta) \\ \dfrac{1}{4m^2}(t-\beta) - \dfrac{1}{6}(\chi - t)^3, & t \in [\beta,\chi) \\ \dfrac{1}{4m^2}(t-\beta), & t \in [\chi,1) \\ o, & \text{elsewhere} \end{cases} \tag{8}$$

$$P_{i,4}(t) = \begin{cases} \dfrac{1}{24}(t-\alpha)^4, & t \in [\alpha,\beta) \\ \dfrac{1}{8m^2}(t-\beta)^2 - \dfrac{1}{24}(\chi - x)^4 + \dfrac{1}{192m^4}, & t \in [\beta,\chi) \\ \dfrac{1}{8m^2}(t-\beta)^2 + \dfrac{1}{192m^4}, & t \in [\chi,1) \\ o, & \text{elsewhere} \end{cases} \tag{9}$$

$$P_{i,n}(t)=\begin{cases}\dfrac{1}{n!}(t-\alpha)^n, & t\in[\alpha,\beta)\\ \dfrac{1}{n!}(t-\alpha)^n-\dfrac{2}{n!}(t-\beta)^n, & t\in[\beta,\chi)\\ \dfrac{1}{n!}(t-\alpha)^n-\dfrac{2}{n!}(t-\beta)^n-\dfrac{1}{n!}(t-\chi)^n, & t\in[\chi,1)\\ o, & \text{elsewhere}\end{cases} \tag{10}$$

The quasilinearization process [26] is a popularize Newton-Raphson method for functional equations which converges quadratically to the exact solution.

Consider the non-linear m^{th} order differential equation:

$$L^m v(x)=f\left[v(x),v'(x),\ldots,v^{(m-1)}(x),x\right]$$

where n is the order of the differentiation, stratifying the quasilinearization technique to the previous equation yields:

$$L^m v_{i+1}(x)=f\left[v_i(x),v_i'(x),\ldots,v_i^{(m-1)}(x),x\right]+$$
$$+\sum_{j=0}^{m-1}\left[v_{i+1}^{(j)}(x)-v_i^{(j)}(x)\right]f_{v^{(j)}}\left[v_i(x),v_i'(x),\ldots,v_i^{(m-1)}(x),x\right]$$

a linear differential equation and can be solved periodically, where $v_i(x)$ is known and one can utilize it to gain $v_i(x)$ for $i = 0,1...$, with the initial conditions and boundary conditions at $(i + 1)^{\text{th}}$ iteration.

Modification of Haar wavelet scheme

We describe a new modification of the HWM for solving systems of NPDE equations with help of the initial and boundary conditions and the results are displayed graphically for different value of the adiabatic index. It is known that any integrable function:

$$L(x,y,z,t)\in L^4\left([0,1)\times[0,1)\times[0,1)\times[0,1)\right)$$
$$M(x,y,z,t)\in L^4\left([0,1)\times[0,1)\times[0,1)\times[0,1)\right)$$
$$N(x,y,z,t)\in L^4\left([0,1)\times[0,1)\times[0,1)\times[0,1)\right)$$
$$Q(x,y,z,t)\in L^4\left([0,1)\times[0,1)\times[0,1)\times[0,1)\right)$$
$$P(x,y,z,t)\in L^4\left([0,1)\times[0,1)\times[0,1)\times[0,1)\right)$$

can be expanded by a Haar series with an infinite number of terms:

$$L(x,y,z,t)=\sum_{i=1}^{\infty}\sum_{j=1}^{\infty}\sum_{k=1}^{\infty}\sum_{s=1}^{\infty}a_{i,j,k,s}h_i(x)h_j(y)h_k(z)h_s(t)$$

$$M(x,y,z,t)=\sum_{i=1}^{\infty}\sum_{j=1}^{\infty}\sum_{k=1}^{\infty}\sum_{s=1}^{\infty}b_{i,j,k,s}h_i(x)h_j(y)h_k(z)h_s(t)$$

$$N(x,y,z,t)=\sum_{i=1}^{\infty}\sum_{j=1}^{\infty}\sum_{k=1}^{\infty}\sum_{s=1}^{\infty}c_{i,j,k,s}h_i(x)h_j(y)h_k(z)h_s(t)$$

$$Q(x,y,z,t)=\sum_{i=1}^{\infty}\sum_{j=1}^{\infty}\sum_{k=1}^{\infty}\sum_{s=1}^{\infty}d_{i,j,k,s}h_i(x)h_j(y)h_k(z)h_s(t)$$

$$P(x,y,z,t)=\sum_{i=1}^{\infty}\sum_{j=1}^{\infty}\sum_{k=1}^{\infty}\sum_{s=1}^{\infty}e_{i,j,k,s}h_i(x)h_j(y)h_k(z)h_s(t)$$

We can be expressed as $W_{2M\times 2M}(yz) = H_{2M}(y)H^T_{2M}(z)$.The aforementioned series terminate at finite terms if $L(x, y, z, t)$, $M(x, y, z, t)$, $N(x, y, z, t)$, and $Q(x, y, z, t)$ are piecewise constant functions or can be approximated as piecewise constant functions during each subinterval, then $L(x, y, z, t)$, $M(x, y, z, t)$, $N(x, y, z, t)$, and $Q(x, y, z, t)$ will be terminated at finite terms, *i. e*:

$$L(x,y,z,t)=\sum_{i=1}^{2M}\sum_{j=1}^{2M}\sum_{k=1}^{2M}\sum_{s=1}^{2M}a_{i,j,k,s}h_i(x)h_j(y)h_k(z)h_s(t)=$$
$$=H^T_{2M}(x)A_{2M\times 2M}W_{2M\times 2M}(yz)H_{2M}(t) \tag{11}$$

$$M(x,y,z,t)=\sum_{i=1}^{2M}\sum_{j=1}^{2M}\sum_{k=1}^{2M}\sum_{s=1}^{2M}b_{i,j,k,s}h_i(x)h_j(y)h_k(z)h_s(t)=$$
$$=H^T_{2M}(x)B_{2M\times 2M}W_{2M\times 2M}(yz)H_{2M}(t) \tag{12}$$

$$N(x,y,z,t)=\sum_{i=1}^{2M}\sum_{j=1}^{2M}\sum_{k=1}^{2M}\sum_{s=1}^{2M}c_{i,j,k,s}h_i(x)h_j(y)h_k(z)h_s(t)=$$
$$=H^T_{2M}(x)C_{2M\times 2M}W_{2M\times 2M}(yz)H_{2M}(t) \tag{13}$$

$$\rho(x,y,z,t)=\sum_{i=1}^{2M}\sum_{j=1}^{2M}\sum_{k=1}^{2M}\sum_{s=1}^{2M}d_{i,j,k,s}h_i(x)h_j(y)h_k(z)h_s(t)=$$
$$=H^T_{2M}(x)D_{2M\times 2M}W_{2M\times 2M}(yz)H_{2M}(t) \tag{14}$$

$$P(x,y,z,t)=\sum_{i=1}^{2M}\sum_{j=1}^{2M}\sum_{k=1}^{2M}\sum_{s=1}^{2M}e_{i,j,k,s}h_i(x)h_j(y)h_k(z)h_s(t)=$$
$$=H^T_{2M}(x)E_{2M\times 2M}W_{2M\times 2M}(yz)H_{2M}(t) \tag{15}$$

where the coefficients $A_{2M\times 2M}$, $B_{2M\times 2M}$, $C_{2M\times 2M}$, $D_{2M\times 2M}$, and the Haar function vectors $H^T_{2M}(y)$, $H_{2M}(z)$ are defined:

$$H^T_{2M}(x)=\left[h_1(x),h_2(x),\ldots,h_{2M}(x)\right],\quad H_{(2M)}(y)=\left[h_1(y),h_2(y),\ldots,h_{2M}(y)\right]^T$$

$$H^T_{2M}(z)=\left[h_1(z),h_2(z),\ldots,h_{2M}(z)\right],\quad H_{(2M)}(t)=\left[h_1(t),h_2(t),\ldots,h_{2M}(t)\right]^T$$

$$W_{(2M\times 2M)}(yz)=H_{2M}(y)H_{2M}^{T}(z),\ A_{(2M\times 2M)}=\left(a_{i,j,k,s}\right)_{2M\times 2M}$$
$$B_{(2M\times 2M)}=\left(b_{i,j,k,s}\right)_{2M\times 2M}$$
$$C_{(2M\times 2M)}=\left(c_{i,j,k,s}\right)_{2M\times 2M},\ \text{and}\ D_{(2M\times 2M)}=\left(d_{i,j,k,s}\right)_{2M\times 2M}$$

We apply the modified HWM to solve the 4-D system of NPDE (1) with the initial and boundary conditions:

$$L(x,y,z,0)=f_1(x,y,z),\ L(x,y,0,t)=s_1(x,y,t),\ L(x,0,z,t)=w_1(x,z,t)$$
$$L(0,y,z,t)=r_1(y,z,t),\ L(0,0,0,t)=e_1(t) \tag{16}$$

$$M(x,y,z,0)=f_2(x,y,z),\ M(x,y,0,t)=s_2(x,y,t),\ M(x,0,z,t)=w_2(x,z,t)$$
$$M(0,y,z,t)=r_2(y,z,t),\ M(0,0,0,t)=e_2(t) \tag{17}$$

$$N(x,y,z,0)=f_3(x,y,z),\ N(x,y,0,t)=s_3(x,y,t),\ N(x,0,z,t)=w_3(x,z,t)$$
$$N(0,y,z,t)=r_3(y,z,t),\ N(0,0,0,t)=e_3(t) \tag{18}$$

$$\rho(x,y,z,0)=f_4(x,y,z),\ \rho(x,y,0,t)=s_4(x,y,t),\ \rho(x,0,z,t)=w_4(x,z,t)$$
$$\rho(0,y,z,t)=r_4(y,z,t),\ \rho(0,0,0,t)=e_4(t) \tag{19}$$

$$P(x,y,z,0)=f_5(x,y,z),\ P(x,y,0,t)=s_5(x,y,t),\ P(x,0,z,t)=w_5(x,z,t)$$
$$P(0,y,z,t)=r_5(y,z,t),\ P(0,0,0,t)=e_5(t) \tag{20}$$

where the previous functions are got from the exact solution in [2] and $0\le x\le 1$, $0\le y\le 1$, $0\le z\le 1$, and $0\le t\le 1$.

First, we consider the first equation of system (1), with the initial and boundary conditions (16). We assume that $\dot{L}'^{*\bullet}(x, y, z, t)$ can be expanded in terms of Haar wavelets as:

$$\dot{L}'^{*\bullet}(x,y,z,t)=\sum_{i=1}^{2M}\sum_{j=1}^{2M}\sum_{k=1}^{2M}\sum_{s=1}^{2M}a_{i,j,k,s}h_i(x)h_j(y)h_k(z)h_s(t) \tag{21}$$

where dot, prime, star and closed circle mean differentiation with respect to t, x, y, and z, respectively.

We integrate (21) one time with respect to t on $[0, t]$, then one time with respect to x on [0. x], one time with respect to y on $[0, y]$, and finally one time with respect to z on $[0, z]$. These, respectively, yield:

$$L'^{*\bullet}(x,y,z,t)=\sum_{i=1}^{2M}\sum_{j=1}^{2M}\sum_{k=1}^{2M}\sum_{s=1}^{2M}a_{i,j,k,s}p_{s,1}(t)h_i(x)h_j(y)h_k(z)+$$
$$L'^{*\bullet}(x,y,z,0)-L'^{*\bullet}(x,y,z,t) \tag{22}$$

$$L^{*\bullet}(x,y,z,t)=(t-t_s)\sum_{i=1}^{2M}\sum_{j=1}^{2M}\sum_{k=1}^{2M}\sum_{s=1}^{2M}a_{i,j,k,s}\,p_{s,1}(t)\,p_{i,1}(x)h_j(y)h_k(z)+\ L^{*\bullet}(x,y,z,0)-$$
$$-L^{*\bullet}(x,y,z,t)+L^{*\bullet}(0,y,z,0)-L^{*\bullet}(0,y,z,t) \tag{23}$$

$$L^{\bullet}(x,y,z,t)=\sum_{i=1}^{2M}\sum_{j=1}^{2M}\sum_{k=1}^{2M}\sum_{s=1}^{2M}a_{i,j,k,s}p_{s,1}(t)\,p_{i,1}(x)\,p_{j,1}(y)h_k(z)+L^{\bullet}(x,y,z,0)-$$
$$-L^{\bullet}(x,y,z,t)+L^{\bullet}(x,0,z,0)-L^{\bullet}(x,0,z,t)+L^{\bullet}(0,y,z,0)-$$
$$-L^{\bullet}(0,y,z,t)+\ L^{\bullet}(0,0,z,0)-L^{\bullet}(0,0,z,t) \tag{24}$$

$$L'^{*\bullet}(x,y,z,t)=\sum_{i=1}^{2M}\sum_{j=1}^{2M}\sum_{k=1}^{2M}\sum_{s=1}^{2M}a_{i,j,k,s}\,p_{s,1}(t)\,h_i(x)h_j(y)h_k(z)+$$
$$L'^{*\bullet}(x,y,z,0)-L'^{*\bullet}(x,y,z,t) \tag{25}$$

Now, individual differentiation of (25) with respect to t, x, y, and z, separately, yield:

$$\dot{L}(x,y,z,t)=\sum_{i=1}^{2M}\sum_{j=1}^{2M}\sum_{k=1}^{2M}\sum_{s=1}^{2M}a_{i,j,k,s}h_i(t)\,p_{i,1}(x)\,p_{j,1}(y)\,p_{k,1}(z)-\dot{L}(x,y,z,t)-$$
$$-\dot{L}(0,y,z,t)-\dot{L}(x,0,z,t)-\dot{L}(x,y,0,t)-\dot{L}(0,0,0,t) \tag{26}$$

$$L'(x,y,z,t)=\sum_{i=1}^{2M}\sum_{j=1}^{2M}\sum_{k=1}^{2M}\sum_{s=1}^{2M}a_{i,j,k,s}\,p_{s,1}(t)h_{i,1}(x)\,p_{j,1}(y)\,p_{k,1}(z)+L'(x,y,z,0)-$$
$$-L'(x,y,z,t)+L'(x,0,z,0)-L'(x,0,z,t)+L'(x,y,0,0)-L'(x,y,0,t) \tag{27}$$

$$L^{*}(x,y,z,t)=\sum_{i=1}^{2M}\sum_{j=1}^{2M}\sum_{k=1}^{2M}\sum_{s=1}^{2M}a_{i,j,k,s}\,p_{s,1}(t)\,p_{i,1}(x)h_i(y)\,p_{k,1}(z)+L^{*}(x,y,z,0)-$$
$$-L^{*}(x,y,z,t)+L^{*}(0,y,z,0)-L^{*}(0,y,z,t)+L^{*}(x,y,0,0)-L^{*}(x,y,0,t) \tag{28}$$

$$L^{\bullet}(x,y,z,t)=\sum_{i=1}^{2M}\sum_{j=1}^{2M}\sum_{k=1}^{2M}\sum_{s=1}^{2M}a_{i,j,k,s}\,p_{s,1}(t)\,p_{i,1}(x)\,p_{j,1}(y)h_i(z)+L^{\bullet}(x,y,z,0)-$$
$$-L^{\bullet}(x,y,z,t)+L^{\bullet}(0,y,z,0)-L^{\bullet}(0,y,z,t)+L^{\bullet}(x,0,z,0)-L^{\bullet}(x,0,z,t) \tag{29}$$

There are a few conceivable outcomes for treating the non-linearity in eq. (1). But, here the quasi-linearization procedure [26] is utilized to handle the non-linearity in eq. (1). The system of (1) trailed by the quasi-linearization prompts to:

$$\rho(x,y,z,t)+\rho(x,y,z,t)\Big[L'(x,y,z,t)+M\ \ (x,y,z,t)+L^{\bullet}(x,y,z,t)\Big]+$$
$$L(x,y,z,t)\rho'(x,y,z,t)+M(x,y,z,t)\rho\ \ (x,y,z,t)\quad N(x,y,z,t)\rho^{\bullet}(x,y,z,t)=0$$

$$\dot{L}(x,y,z,t)+L(x,y,z,t)L'(x,y,z,t)+M(x,y,z,t)L^{*}(x,y,z,t)+$$
$$+N(x,y,z,t)L^{\bullet}(x,y,z,t)+\frac{1}{\rho}p'(x,y,z,t)=0$$

$$\dot{M}(x,y,z,t)+L(x,y,z,t)M'(x,y,z,t)+M(x,y,z,t)M^{*}(x,y,z,t)+$$
$$+N(x,y,z,t)M^{\bullet}(x,y,z,t)+\frac{1}{\rho(x,y,z,t)}P^{*}(x,y,z,t)=0$$

$$\dot{N}(x,y,z,t)+M(x,y,z,t)N'(x,y,z,t)+N(x,y,z,t)N^{*}(x,y,z,t)+ \tag{30}$$
$$+N(x,y,z,t)N^{\bullet}(x,y,z,t)+\frac{1}{\rho(x,y,z,t)}P^{\bullet}(x,y,z,t)=0$$

$$\dot{P}(x,y,z,t)+\gamma P(x,y,z,t)\left[L'(x,y,z,t)+M^{*}(x,y,z,t)+N^{\bullet}(x,y,z,t)\right]+L(x,y,z,t)P'(x,y,z,t)+$$
$$+M(x,y,z,t)P^{*}(x,y,z,t)+N(x,y,z,t)P^{\bullet}(x,y,z,t)=0$$

Now, discretizing the result (30) by $x \to x_l$, $y \to y_l$, $z \to z_l$, $t \to t_l$, and using eqs. (26)-(29) and discretizing using the collocation points $x_l = y_l = z_l = t_l = (l - 0.5)/2M$, $l = 1..2M$ yield a non-linear system of algebraic equations, with the initial and boundary conditions and the wavelets coefficients $a_{i,j,k,s}$, $b_{i,j,k,s}$, $c_{i,j,k,s}$, $d_{i,j,k,s}$, and $e_{i,j,k,s}$, can be successively calculated for all i, j, k, and s. Further, putting the computed wavelets coefficients $a_{i,j,k,s}$, $b_{i,j,k,s}$, $c_{i,j,k,s}$, $d_{i,j,k,s}$, and $e_{i,j,k,s}$ into eqs. (11)-(15), we can successively calculate the approximate solutions at different times.

Discussion of the results

We present the numerical solutions of the system of unsteady gas-flow in 4-D (1), The analytical solutions are taken from [2] as:

$$L(x,y,z,t)=\frac{-\sqrt{2c_3-c_4^2}\,y+c_4x+c_3t\,x}{c_3t^2+2c_4\,t+2},\quad M(x,y,z,t)=\frac{\sqrt{2c_3-c_4^2}\,x+c_4y+c_3t\,y}{c_3t^2+2c_4\,t+2}$$

$$N(x,y,z,t)=\frac{z+c_2+\tan^{-1}\left(\dfrac{y}{x}\right)-\tan^{-1}\left(\dfrac{c_3\,t+c_4}{\sqrt{2c_3-c_4^2}}\right)}{t+1}$$

$$Q(x,y,z,t)=\frac{C_5}{(t+1)\left(y^2+x^2\right)},\quad P(x,y,z,t)=\frac{C_1}{(t+1)^{\gamma}\left(C_3\,t^2+2C_4t+2\right)^{\gamma}}$$

In figs. 1-3 show representations of velocity component profiles (L, M, and N), respectively, indicating a decay in velocity during time increment and an increase with a spatial direction x, y, and increment, respectively. The largest velocity component was achieved by M and N while the largest increase with a spatial variable was achieved by L.

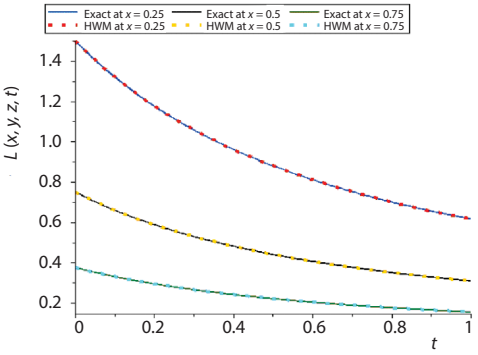

Figure 1. Comparison of the velocity component (L) at $C_3 = C_4 = 1$ at $y = 0$ by HWM and the analytical solutions in [2]
(*for color image see journal web site*)

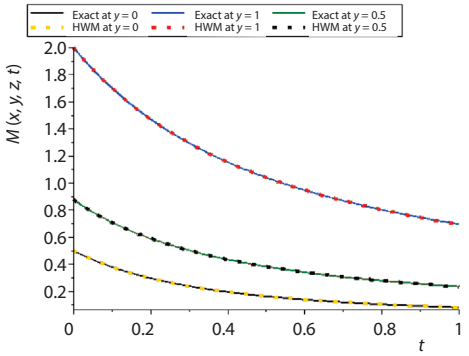

Figure 2. Comparison of the velocity component (M) plot at $C_3 = C_4 = 1$ at $y = 0$ by HWM and the analytical solutions in [2]
(*for color image see journal web site*)

Figure 3 illustrates velocity profile N showing effect of velocity value with increasing the time. In fig. 4, showing effect of with increasing x. Figure 5 showing the effect adiabatic index and this is just as it exists in reference [2].

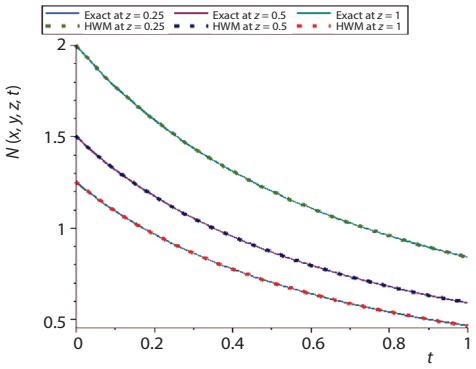

Figure 3. Comparison of the velocity component (N) plot at $C_3 = C_4 = 1$ at $y = 0$ by HWM and the analytical solutions in [2]
(*for color image see journal web site*)

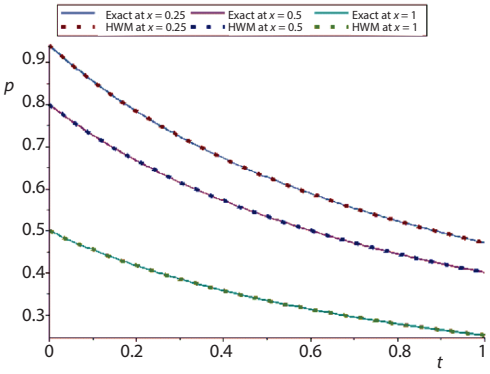

Figure 4. Comparison of the density compilation at $C_5 = 1$ by HWM and the dual vector combination analytical solutions in [2]
(*for color image see journal web site*)

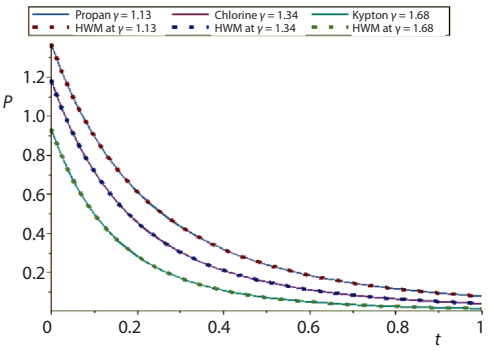

Figure 5. Comparison of the pressure compilation at $C_1 = C_2 = C_3 = C_4 = C_5 = 1$ at $\gamma = 1.13$, $\gamma = 1.34$, $\gamma = 1.68$ by HWM and the analytical solutions in [2]
(*for color image see journal web site*)

In tab. 1 show the comparison of approximate solutions of the 4-D system of the unsteady gas-flow (1) obtained by using the modified HWM with the analytical solutions in [2] at $(x, y, z) = (1, 1, 1)$.

Table 1. Comparison between the approximate solutions using HWM at $M = 4$ and the analytical solutions in [2]

t	Absolute errors of L	Absolute errors of M	Absolute errors of N	Absolute errors of P	Absolute errors of ρ
0.1	$2.16 \cdot 10^{-6}$	$6.322 \cdot 10^{-6}$	$1.201 \cdot 10^{-6}$	$3.025 \cdot 10^{-6}$	$3.321 \cdot 10^{-6}$
0.2	$1.065 \cdot 10^{-6}$	$5.102 \cdot 10^{-6}$	$4.302 \cdot 10^{-6}$	$4.156 \cdot 10^{-6}$	$6.254 \cdot 10^{-6}$
0.3	$3.102 \cdot 10^{-6}$	$4.021 \cdot 10^{-6}$	$4.142 \cdot 10^{-6}$	$2.216 \cdot 10^{-6}$	$4.358 \cdot 10^{-6}$
0.4	$4.015 \cdot 10^{-6}$	$3.250 \cdot 10^{-6}$	$3.306 \cdot 10^{-6}$	$1.541 \cdot 10^{-6}$	$6.024 \cdot 10^{-6}$
0.5	$3.025 \cdot 10^{-6}$	$4.203 \cdot 10^{-6}$	$1.512 \cdot 10^{-6}$	$1.487 \cdot 10^{-6}$	$4.254 \cdot 10^{-6}$
0.6	$2.96 \cdot 10^{-6}$	$3.021 \cdot 10^{-6}$	$6.325 \cdot 10^{-6}$	$6.241 \cdot 10^{-6}$	$3.652 \cdot 10^{-6}$
0.7	$3.21 \cdot 10^{-6}$	$2.302 \cdot 10^{-6}$	$1.241 \cdot 10^{-6}$	$4.212 \cdot 10^{-6}$	$3.201 \cdot 10^{-6}$
0.8	$1.36 \cdot 10^{-5}$	$6.215 \cdot 10^{-5}$	$2.021 \cdot 10^{-5}$	$5.275 \cdot 10^{-5}$	$4.021 \cdot 10^{-5}$
0.9	$2.25 \cdot 10^{-5}$	$4.302 \cdot 10^{-5}$	$6.045 \cdot 10^{-5}$	$3.214 \cdot 10^{-5}$	$2.541 \cdot 10^{-5}$

Conclusion

In the perspective on aforementioned numerical precedents, it is presumed that 4-D Haar wavelet technique are progressively solid and precise scientific device for settling the unsteady gas-flow in 4-D. For getting the vital accuracy, the quantity of estimation focuses might be expanded. This technique is totally another plan to unravel the unsteady gas-flow in 4-D. It is a joined methodology and a novel intermingling hypothesis is introduced. It is a stable numerical technique and its strength has been appeared. Setting up the calculation is simple and straight forward. The merit of this strategy is that the maximum absolute errors are diminished by expanding the quantity of collocation points. The proposed plan yields better exactness in examination with the other numerical techniques which are exhibited in [14, 15] accessible in the writing. Calculation can be stretched out to comprehend other frameworks of higher dimensional issues in various regions of physical and numerical sciences.

References

[1] Farzaneh-Gord, M., Rahbari, H. R., Unsteady Natural Gas-Flow Within Pipe-Line Network, an Analytical Approach, *Journal of Natural Gas Science and Engineering*, 28 (2016), Jan., pp. 397-409
[2] Rashed, A. S., Analysis of (3+1)-Dimensional Unsteady Gas-Flow Using Optimal System of Lie Symmetries, Mathematics and Computers in Simulation, *Mathematics and Computers in Simulation*, *156* (2019), C, pp. 327-346
[3] Oliveri, F., Speciale, M. P., Exact Solutions to the Unsteady Equations of Perfect Gases through Lie Group Analysis and Substitution Principles, *Int. J. Non-Linear Mech*., *37* (2002), 2, pp. 257-274
[4] Plotnikov, L., *et al*., The Flows Structure in Unsteady Gas-Flow in Pipes with Different Cross-Sections, *EPJ Web of Conferences 159* (2017), Jan., 00035
[5] Titarev, V. A., Shakhov, E. M., Unsteady Rarefied Gas-Flow with Shock Wave in a Channel, *Fluid Dynamics*, *53* (2018), May, pp. 143-151
[6] Raja Sekhar, T., Sharma, V. D., Similarity Solutions for 3-D Euler Equations Using Lie Group Analysis, *Appl. Math. Comput*., *196* (2008), 1, pp. 147-157
[7] Arbabi, S., *et al*., A 2-D Haar Wavelets Method for Solving System of PDE, *Applied Mathematics and Computation*, *292* (2017), Jan., pp. 33-46

[8] Arnold, A., Numerically Absorbing Boundary Conditions for Quantum Evolution Equations, *VLSI Design*, *6* (1998), ID38298
[9] Celik, I., Haar Wavelet Method for Solving Generalized Burger Huxley Equation, *Arab. Journal of Mathematical Sciences*, *18*, (2012), 1, pp. 25-37
[10] Singh, I., Kumar, S., Haar Wavelet and Adomain Decomposition Method for Solving Third Order Partial Differential Equations Arising in Impulsive Motion of a Flat PlatE, *International Journal of Mathematical Modelling and Computation*, *6* (2016), 2, pp. 175-188
[11] Singh, I., Kumar, S., Wavelet Methods for Solving 3-D Partial Differential Equations, *Mathematical Sciences*, *11* (2017), 2, pp. 145-154
[12] Siraj-ul-Islam, I., *et al*., A Numerical Assessment of Parabolic Partial Differential Equations Using Haar and Legendre Wavelets, *Applied Mathematical Modelling*, *37* (2013), 23, pp. 9455-9481
[13] Kaushik, A., Kumar, A., Numerical Study of Steady 1-D Incompressible Flow Through a Nozzle Using Simple Algorithm, *International Journal of Scientific Research in Mathematical and Statistical Sciences*, *3*, (2016), 5, pp. 1-7
[14] Biazar, J., Eslami, M., A New Homotopy Perturbation Method for Solving Systems of Partial Differential Equations, *Comput. Math. Appl*., *62* (2011), 1, pp. 225-234
[15] Matinfar, M., *et al*., A New Homotopy Analysis Method for Finding the Exact Solution of Systems of Partial Differential Equations, *Selcuk J. Appl. Math*., *13* (2012), 1, pp. 41-56
[16] Yildirim, K., A Solution Method for Solving Systems of Non-Linear PDE, *World Appl. Sci. J*., *18* (2012) 11, pp. 1527-1532
[17] Li, Y., Zhao, W., Haar Wavelet Operational Matrix of Fractional Order Integration and Its Applications in Solving the Fractional Order Differential Equations, *Appl. Math.Comput*., *216* (2010), 8, pp. 2276-2285
[18] Ray, S. S., On Haar Wavelet Operational Matrix of General Order and Its Application for the Numerical Solution of Fractional Bagley-Torvik Equation, *Appl. Math. Comput*., *218* (2012), 9, pp. 5239-5248
[19] Ray, S. S., Patra, A., Haar Wavelet Operational Methods for the Numerical Solutions of Fractional Order Non-Linear Oscillatory Van der Pol System, *Appl. Math. Comput*., *220* (2013), Sept., pp. 659-667
[20] Patra, A., Ray, S. S., The 2-D Haar Wavelet Collocation Method for the Solution of Stationary Neutron Transport Equation in a Homogeneous Isotropic Medium, *Ann. Nucl. Energy*, *70* (2014), Aug., pp. 30-35
[21] Ray, S. S., Gupta, A. K., A 2-D Haar Wavelet Approach for the Numerical Simulations of Time and Space Fractional Fokker-Planck Equations in Modelling of Anomalous Diffusion Systems, *Journal Math.*, *Chem*., *52* (2014), July, pp. 2277-2293
[22] Ray, S. S., Gupta, A. K., An Approach with Haar Wavelet Collocation Method for Numerical Simulations of Modified KdV and Modified Burgers Equations, *Comput. Model. Eng. Sci.*, *103* (2014), 5, pp. 315-341
[23] Yildirim, K., A Solution Method for Solving Systems of Non-Linear PDE, *World Appl. Sci. J*., *18* (2012), 11, pp. 1527-1532
[24] Arbabi, S., *et al*., A Semi-Analytical Solution of Hunter-Saxton Equation, *Optik*, *127* (2016), 13, pp. 5255-5258
[25] Raja Sekhar, T., Sharma, V. D., Similarity Solutions for 3-D Euler Equations Using Lie Group Analysis, *Appl. Math. Comput.*, *196* (2008), 1, pp. 147-157
[26] Bellman, R. E., Kalaba, R. E., *Quasilinearization and Non-Linear Boundary-Value Problems*, American Elsevier Pub. Co., New York, USA, 1965

Paper submitted: January 1, 2019
Paper revised: June 15, 2019
Paper accepted: June 22, 2019